

**Spin-glass state in  $\text{CuGa}_2\text{O}_4$** 

G. A. Petrakovskii, K. S. Aleksandrov, L. N. Bezmaternikh, and S. S. Aplesnin  
*Institute of Physics, Academy of Sciences, Siberian Branch, 660036 Krasnoyarsk, Russia*

B. Roessli and F. Semadeni  
*Laboratory for Neutron Scattering, Paul Scherrer Institute and ETH Zurich, CH-5232 Villigen PSI, Switzerland*

A. Amato and C. Baines  
*Laboratory for Muon-Spin Spectroscopy, Paul Scherrer Institute, CH-5232 Villigen PSI, Switzerland*

J. Bartolomé and M. Evangelisti\*  
*Instituto de Ciencia de Materiales de Aragón, CSIC–Universidad de Zaragoza, Ciudad Universitaria, 50009 Zaragoza, Spain*  
 (Received 10 July 2000; revised manuscript received 6 February 2001; published 20 April 2001)

Magnetic susceptibility, magnetization, specific-heat, and positive muon spin relaxation ( $\mu\text{SR}$ ) measurements have been used to characterize the magnetic ground state of the spinel compound  $\text{CuGa}_2\text{O}_4$ . We observe a spin-glass transition of the  $S=1/2$   $\text{Cu}^{2+}$  spins below  $T_f=2.5$  K characterized by a cusp in the susceptibility curve which is suppressed when a magnetic field is applied. We show that the magnetization of  $\text{CuGa}_2\text{O}_4$  depends on the magnetic history of the sample. Well below  $T_f$ , the muon signal resembles the dynamical Kubo-Toyabe expression reflecting that the spin freezing process in  $\text{CuGa}_2\text{O}_4$  results in a Gaussian distribution of the magnetic moments. By means of Monte Carlo simulations, we obtain the relevant exchange integrals between the  $\text{Cu}^{2+}$  spins in this compound.

DOI: 10.1103/PhysRevB.63.184425

PACS number(s): 75.50.Lk, 76.75.+i, 75.40.Cx, 02.70.Rr

**I. INTRODUCTION**

Although spin glasses have been extensively studied in the past years, there is still no consensus about the ground state and dynamics in these systems (for an introduction, see e.g., K. H. Fisher and J. A. Hertz<sup>1</sup>). It is generally accepted that both site disorder and competition between the magnetic moments are necessary to produce a low-temperature state where the spins are frozen along arbitrary directions.<sup>2</sup> Examples of such systems are metallic spin glasses where magnetic impurities are randomly diluted in a noble metal.<sup>3</sup> For this particular class of materials competition between the magnetic moments is the result of the Rudermann-Kittel-Kasuya-Yosida (RKKY) interaction<sup>4</sup> where ferromagnetic and antiferromagnetic exchange interactions alternate as a function of distance between neighboring spins. The RKKY interaction cannot be invoked for localized magnets and the spin glass transition in these systems must be realized by other mechanisms. Typical insulating spin glasses of this kind are the alloys  $\text{Eu}_x\text{Sr}_{1-x}\text{S}$ . In the  $x=1$  limit,  $\text{EuS}$  is a well-known example of an isotropic three-dimensional Heisenberg ferromagnet. The exchange integrals have been determined by inelastic neutron scattering in this material with the result that ferromagnetic nearest-neighbor exchange interaction competes with next-nearest antiferromagnetic coupling.<sup>5</sup> Diluting nonmagnetic Sr for Eu ensures bond randomness and the conditions for obtaining a spin-glass state are fulfilled in a large range of impurity concentrations,<sup>6</sup> in qualitative agreement with the molecular-field theory of Edwards and Anderson.<sup>7</sup> De Seze pointed out that a spin-glass phase transition can occur in a geometrically frustrated system with Ising spins and antiferromagnetic interactions only.<sup>8</sup> Following De Seze's work, Villain<sup>9</sup> proposed that spin glasses can be obtained in materials with geometric frustration and Heisenberg-type exchange interactions like cubic

spinel. These compounds have the chemical formula  $AB_2O_4$ . The chemical structure of spinels consists of both tetrahedral and octahedral sites. The number of crystallographic sites is larger than the number of  $A$  and  $B$  cations in the chemical formula, so that the cations generally distribute randomly among the available atomic positions. In particular, this random distribution of cations determines in a large extent the microwave relaxation properties of the spinel compounds.<sup>10</sup> When both sublattices are occupied by magnetic ions the ground state is a ferrimagnet. The  $B$  sublattice builds connected tetrahedra and antiferromagnetic interactions induce topological frustrations<sup>11</sup> which can lead to a spin-glass state when nonmagnetic impurities are introduced.<sup>9</sup> The dominant magnetic interaction in most of these materials is antiferromagnetic and connects spins between the  $A$  and  $B$  sublattices while the  $A$ - $A$  and  $B$ - $B$  exchange interactions are comparatively small. However, inter-sublattice exchange constants can modify the magnetic-phase diagram originally calculated by Villain and for real systems the situation is usually complicated.<sup>12</sup> Although spin-glass transition has been found in diluted spinels,<sup>13</sup> a spin-glass state in pure cubic spinels is less common.

In this paper, we report magnetic susceptibility, magnetization measurements in fields up to 50 kOe, specific-heat and muon-spin relaxation ( $\mu\text{SR}$ ) measurements in the cubic spinel  $\text{CuGa}_2\text{O}_4$ . The results show that  $\text{CuGa}_2\text{O}_4$  undergoes a paramagnetic to spin-glass phase transition at  $T_f=2.5$  K. By means of Monte Carlo simulations, the relevant exchange interactions are obtained for  $\text{CuGa}_2\text{O}_4$ . We show that the formation of a spin-glass ground state in  $\text{CuGa}_2\text{O}_4$  is probably due to the Jahn-Teller character of the  $\text{Cu}^{2+}$  ions. Specifically, in a field of octahedral symmetry, the Jahn-Teller effect distorts the electronic  $d$  levels of the  $\text{Cu}^{2+}$  which become split by the effect of the crystal field into a threefold

degenerate level and a twofold degenerate one. In such compounds there is an interaction between the electronic system with the underlying lattice which very often leads to a structural phase transition. Typical compounds exhibiting cooperative Jahn-Teller distortion are found in, e.g., perovskites ( $\text{KCuF}_3$ ,  $\text{LaMnO}_3$ ), spinels ( $\text{CuFe}_2\text{O}_4$ ,  $\text{Mn}_3\text{O}_4$ ), rutiles ( $\text{CrF}_2$ ,  $\text{CuF}_2$ ), or garnets ( $\text{Ca}_3\text{Fe}_2\text{Ge}_3\text{O}_{12}$ ). The structural phase transition can be accompanied by orbital ordering of the  $d$  electrons which in turn influences the nature of the exchange interaction. The important role of the Jahn-Teller effect in forming the magnetic ground state in the perovskite manganites which exhibit colossal magnetoresistance (e.g., see Ref. 14 and references therein) and in cuprates (e.g., Refs. 15 and 16 and references therein) is currently a subject of intense investigation both theoretically and experimentally. In that respect, we note that the influence of the Jahn-Teller effect on the properties of the magnetic insulators is discussed in detail by Kugel and Khomsky.<sup>17</sup>

## II. EXPERIMENTAL DETAILS

### A. Sample preparation

Single crystals of  $\text{CuGa}_2\text{O}_4$  were grown by spontaneous crystallization starting from a  $\text{CuO-Ga}_2\text{O}_3$  solution melt in  $\text{PbO-0.64B}_2\text{O}_3\text{-0.5Na}_2\text{O}$ . After slowly cooling the melt to room temperature, single crystals of typical size  $3 \times 3 \times 3 \text{ mm}^3$  and of octahedral shape were obtained. X-ray-diffraction analysis showed that the  $\text{CuGa}_2\text{O}_4$  crystals used for the present experiments are cubic spinels with both copper and gallium ions randomly distributed in the  $A$  and  $B$  sublattices in agreement with previous diffraction investigation (see Ref. 18). The chemical structure of  $\text{CuGa}_2\text{O}_4$  is described by the space group  $Fd\bar{3}m$  with lattice constants  $a = 8.39 \text{ \AA}$  at room temperature.

### B. Magnetic measurements

The magnetic susceptibility and magnetization measurements were performed with a commercial MPMS Quantum Design superconducting quantum interference device (SQUID) magnetometer together with an ac-susceptibility option at ICMA, Spain. The amplitude of the ac-magnetic field was set to 4.5 Oe with the frequency of the field being varied between 1 and 990 Hz. The measurements were carried out in the temperature range 1.7–300 K and in applied magnetic fields up to 50 kOe. Additional measurements of the magnetic susceptibility in the temperature range  $T = 4.2\text{--}120 \text{ K}$  were performed at the Institute of Physics, Krasnoyarsk, using a home-built SQUID magnetometer.

### C. Specific-heat measurements

The specific-heat measurements were performed with a commercial PPMS device (Quantum Design) in the temperature range  $1.8 \leq T \leq 10 \text{ K}$ . We used a small single crystal of mass  $\sim 4.15 \text{ mg}$ . The raw data were corrected for the copper host and glue, which were measured separately. We did not attempt to subtract the phonon contribution, as it is expected to be small at low temperatures.

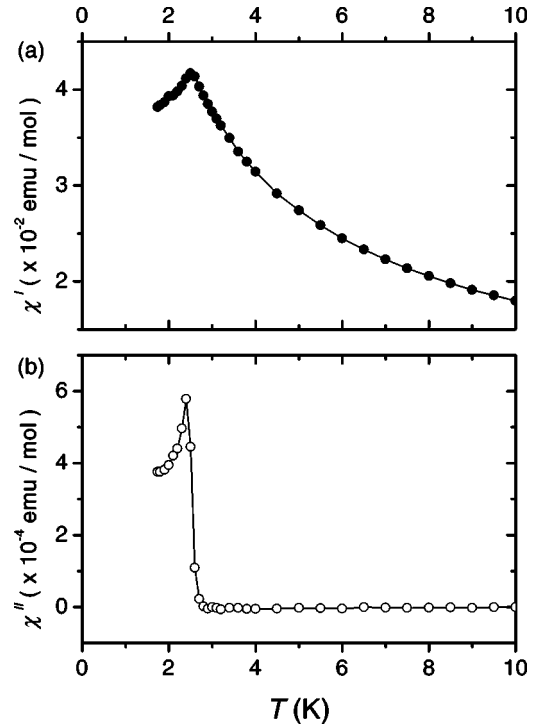


FIG. 1. (a) Real and (b) imaginary parts of the magnetic susceptibility in a single crystal of  $\text{CuGa}_2\text{O}_4$  measured along the  $[001]$  axis. The exciting frequency was 1 Hz, the ac field amplitude 4.5 Oe and the bias applied field  $H = 0 \text{ T}$ .

### D. Muon-spin relaxation

The  $\mu\text{SR}$  experiments were performed on the LTF spectrometer at the Paul-Scherrer Institute, Switzerland. The data were recorded using the zero-field method which is very sensitive to determine both static and dynamic effects in spin glasses.<sup>21,22</sup> Additional measurements were performed as a function of applied magnetic field. In that case, the sample was zero-field cooled. The sample we used for the present experiment consists of about 50 pieces of the above-described crystals which were glued on a silver plate. The sample was enclosed in a top-loading  $^3\text{He-}^4\text{He}$  dilution cryostat and the measurements were carried out in the temperature range  $650 \text{ mK} \leq T \leq 10 \text{ K}$ .

## III. MAGNETIZATION, SUSCEPTIBILITY, AND SPECIFIC-HEAT RESULTS

Figure 1 shows the result of the magnetic-susceptibility measurements with an ac frequency of 1 Hz and an excitation amplitude of  $H = 4.5 \text{ Oe}$ . For temperatures higher than  $T = 20 \text{ K}$ , the magnetic susceptibility is well reproduced by the Curie-Weiss law. Upon lowering the temperature below  $T = 20 \text{ K}$ , the magnetic susceptibility increases continuously. The real part of the magnetic susceptibility shows a cusp at  $T_f \approx 2.5 \text{ K}$  which is independent of the relative orientation of the magnetic field with respect to the crystal axes. The imaginary part of the magnetic susceptibility also exhibits a maximum at the same temperature. To understand the nature of the maxima appearing in the susceptibility curves, the magnetization in  $\text{CuGa}_2\text{O}_4$  was determined as a function of

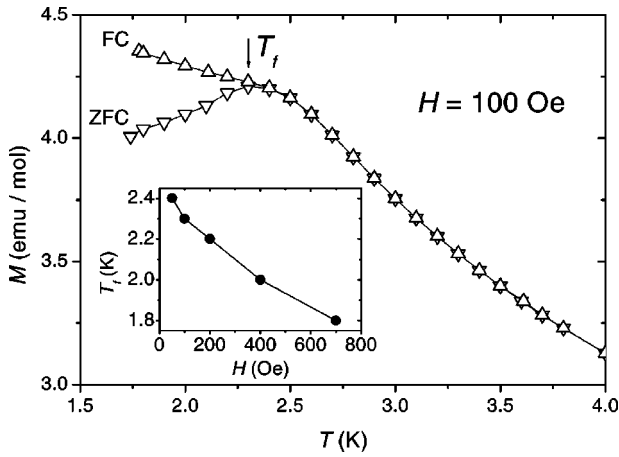


FIG. 2. Temperature dependence of the magnetization of  $\text{CuGa}_2\text{O}_4$  single crystal along the the [001] axis for a sample cooled in zero field (ZFC) and cooled in an applied magnetic field  $H$  (FC). Both curves are measured at a bias field of same value  $H$ . The curves diverge below  $T_f$ . Inset: The bifurcation point tends to lower temperature for increasing bias field.

applied magnetic field and for different magnetic histories of the samples. As an example, Fig. 2 shows the magnetization curves obtained in  $\text{CuGa}_2\text{O}_4$  after zero-field cooling (ZFC) and field cooling (FC), respectively. For the latter case, the sample was cooled in a magnetic field of  $H = 100$  Oe applied along the [001] crystal axis. It is evident from the figure that for temperatures below  $T_f = 2.5$  K, the FC and ZFC magnetization curves show a bifurcation due to thermal hysteresis or irreversibility. This is a usual characteristic for the formation of a spin-glass state. For increasing bias fields the bifurcation temperature tends to lower temperatures, as expected for a spin glass. The results of the magnetic susceptibility measurements taken for different magnetic fields are presented in Fig. 3 which shows that magnetic fields larger than  $H = 5$  kOe suppress the cusp observed at  $T_f$  in zero-magnetic

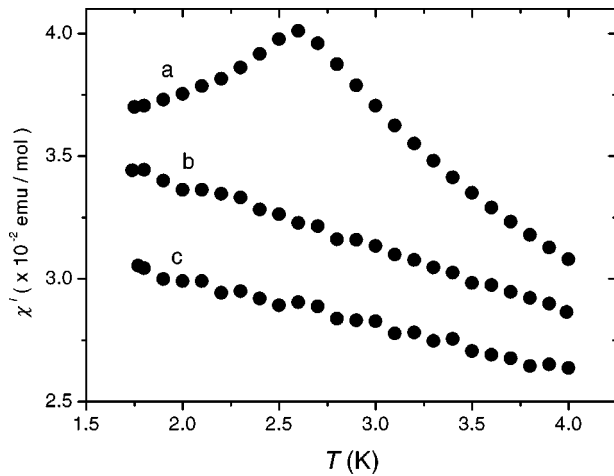


FIG. 3. Temperature dependence of the real component of the ac susceptibility measured at the frequency of 19 Hz and a bias field of (a)  $H = 0$  kOe, (b)  $H = 5$  kOe, and (c)  $H = 10$  kOe.

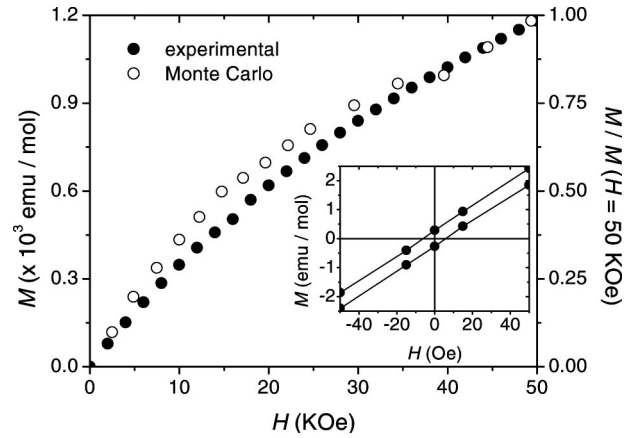


FIG. 4. Magnetization as a function of field. Full symbols: experimental data measured at  $T = 1.8$  K; open symbols: Monte Carlo simulations calculated at the same temperature and parameters given in Sec. VI. Inset: hysteresis loop in the vicinity of the origin.

field. Figure 4 shows that the increase of the magnetic moment as a function of magnetic field at  $T = 1.8$  K is far from saturation at the maximum field of 50 kOe, and in the inset the small, but non-negligible, magnetic hysteresis is also depicted. Both features are characteristic in spin-glass phases. In Fig. 5 the temperature dependence of the transition temperature  $T_f$  of the spin-glass transition is observed to increase as a function of increasing ac frequency. The above experimental results all indicate that the  $\text{Cu}^{2+}$  magnetic moments in  $\text{CuGa}_2\text{O}_4$  undergo a phase transition to a spin-glass ground state below  $T_f \approx 2.5$  K. This is also confirmed by the calorimetric measurements performed in zero-magnetic field for this compound. A plot of the specific heat  $C_p/T$  in  $\text{CuGa}_2\text{O}_4$  is shown in Fig. 6. The data do not show any indication of a phase transition to a three-dimensional ferro-magnetic or antiferromagnetic ordered state. However, a broad maximum is observed around  $T = 2.5$  K followed by a slow decay toward high temperatures. This particular behav-

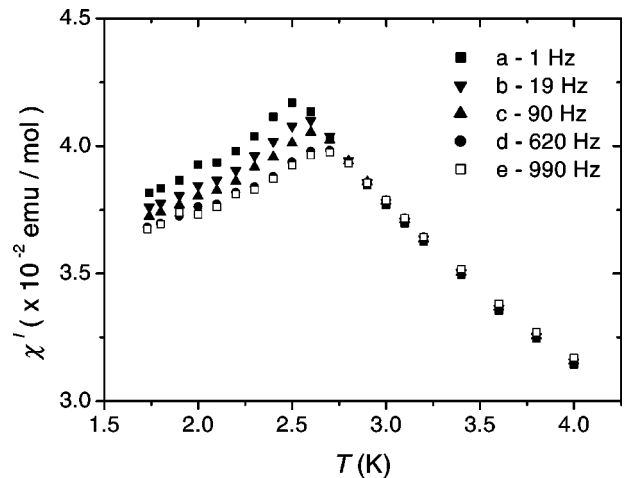


FIG. 5. Magnetic susceptibility measured in  $\text{CuGa}_2\text{O}_4$  along the [001] axis for different frequencies. See text for details.

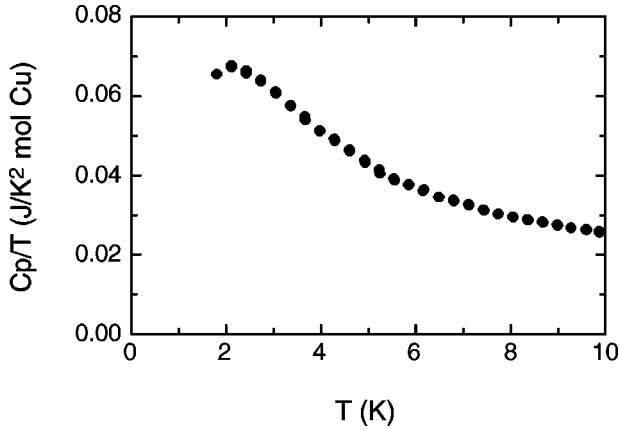


FIG. 6. Specific heat of  $\text{CuGa}_2\text{O}_4$ . The data were not corrected for phonon contribution.

ior of the specific heat as a function of temperature is reminiscent of a spin-glass transition.<sup>19</sup>

#### IV. DISCUSSION OF THE BULK MEASUREMENTS

A spin-glass state is characterized by an assembly of magnetic moments which are frozen along random and arbitrary directions in space below a specific transition temperature  $T_f$ . Because of the nonergodicity of the system, the phenomenon is irreversible. The macroscopic magnetization of a spin-glass system is equal to zero in the absence of a magnetic field. On the other hand, cooling a spin glass in an external magnetic field transfers the system into a metastable state with a nonzero magnetization value. For temperatures above the spin-freezing temperature  $T_f$ , the magnetic moments are in a paramagnetic state and consequently the temperature dependence of the magnetic susceptibility follows the Curie-Weiss law

$$\chi(T) = \frac{C}{T - \theta}, \quad (1)$$

where  $C = Ng^2\mu_B^2S(S+1)/3k_B$  is the Curie constant and  $\theta$  the paramagnetic Curie temperature.  $N$  is the magnetic moment density,  $g$  the Landé factor, and  $\mu_B$  the Bohr magneton.  $S$  corresponds to the spin value of  $\text{Cu}^{2+}$  and  $k_B$  is the Boltzmann constant. From the magnetic susceptibility measurements presented above, we obtain for  $\text{CuGa}_2\text{O}_4$  the values  $C = 0.34$  emu K/mol,  $\theta = -8$  K which implies  $\mu_{\text{eff}} = g\sqrt{S(S+1)}\mu_B = 1.65\mu_B$  with  $g = 1.90$  and  $S = 1/2$ . The magnetic susceptibility is related to the Edwards-Anderson (EA) parameter<sup>7</sup>  $q = \lim_{t \rightarrow \infty} [\langle S_i(t)S_i(0) \rangle]_{\text{av}}$ , through the relation

$$\chi(T) = C \frac{1 - q(T)}{T - \theta[1 - q(T)]}. \quad (2)$$

According to the percolation theory of Kirkpatrick,<sup>20</sup> the EA parameter follows a power law  $q(T) \propto (1 - T/T_f)^{\beta_0}$  close to the spin-glass temperature  $T_f$  with  $\beta_0$  equal to 0.39. However, near  $T_f$ , we found the value  $\beta_0 = 0.16$  in  $\text{CuGa}_2\text{O}_4$ . The frequency dependence of the spin freezing temperature  $T_f$  is a characteristic feature of the spin-glass state. It has

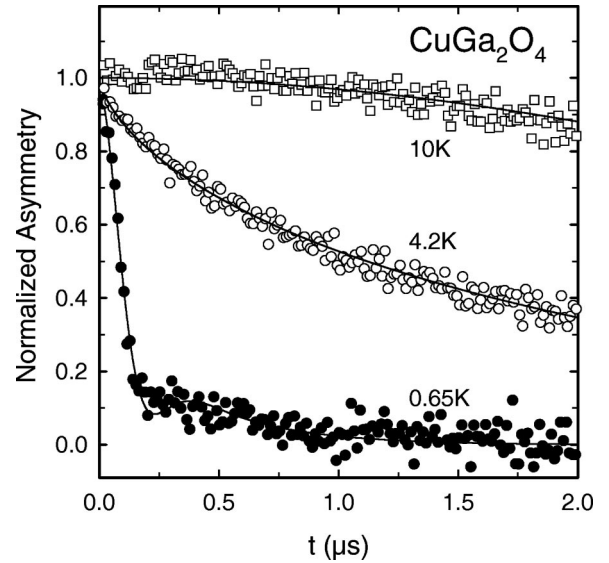


FIG. 7. Experimental zero-field  $\mu\text{SR}$  signal measured in  $\text{CuGa}_2\text{O}_4$  at  $T = 10$  K,  $T = 4.5$  K, and  $T = 650$  mK. The lines represent fits as explained in the text.

been experimentally found that in spin glasses  $T_f$  increases with increasing ac frequency. A quantitative measure of the frequency shift is obtained from  $(\Delta T_f/T_f)/\Delta \ln(\omega) = 0.026$ . It is five times larger than the rate for a metallic spin glass and an order of magnitude smaller than for a superparamagnet.<sup>21</sup>

#### V. $\mu\text{SR}$ RESULTS

To get more insight into both the static and dynamic properties of the  $\text{Cu}^{2+}$  magnetic moments in  $\text{CuGa}_2\text{O}_4$ , we have measured the muon-spin relaxation above and below the freezing temperature  $T_f$  in this material. Generally, the magnetic interactions probed by the implanted spin-polarized muon are detected by monitoring the asymmetric emission of positrons arising from the weak decay of the muon. Recording the positron rate  $N(t)$  as a function of muon lifetime yields

$$N(t) = N(0) \exp(-t/\tau) [1 + AG_z(t)], \quad (3)$$

where  $A$  is the initial muon asymmetry parameter. The product  $AG_z(t)$  is often called the  $\mu\text{SR}$  signal. In addition, the function  $G_z(t)$  can be associated with the muon-spin auto-correlation function, i.e.,

$$G_z(t) = \frac{\langle \mathbf{S}(t)\mathbf{S}(0) \rangle}{S^2(0)}, \quad (4)$$

where  $\mathbf{S}$  is the spin of the muon. Typical zero-field  $\mu\text{SR}$  signals measured in  $\text{CuGa}_2\text{O}_4$  are shown in Fig. 7. Above  $T \approx 3.8$  K (and at least up to 10 K), the data are best described by assuming for  $G_z(t)$  the form

$$G_{z,\text{para}}(t) = G_{KT}(t) \cdot G_{es}(t), \quad (5)$$

with  $G_{KT}$  representing the familiar Kubo-Toyabe (KT) expression,<sup>24,25</sup>

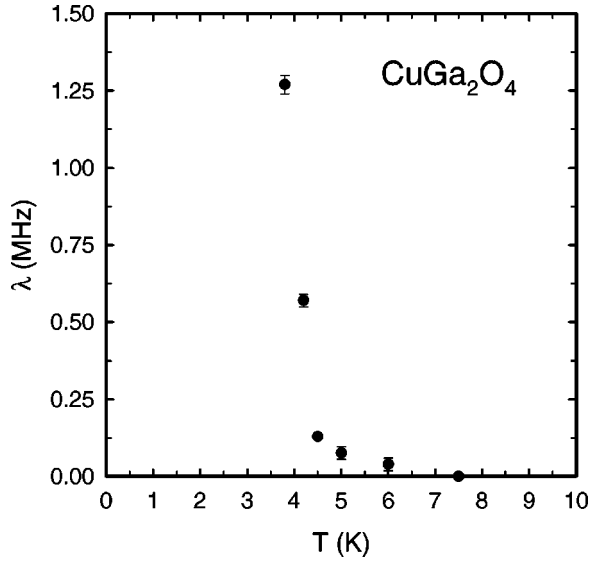


FIG. 8. Temperature dependence of the depolarization rate  $\lambda$  above 3.8 K.

$$G_{KT}(t) = \frac{1}{3} + \frac{2}{3}(1 - \Delta_{ns}^2 t^2) \exp\left(-\frac{1}{2} \Delta_{ns}^2 t^2\right), \quad (6)$$

and with  $G_{es}$  given by

$$G_{es}(t) = \exp[-(\lambda t)^\beta]. \quad (7)$$

The form of  $G_{z,para}(t)$  points for the occurrence of two independent channels of depolarization acting on the muon spin. The first channel, giving rise to the KT function  $G_{KT}$ , originates from the nuclear dipole moments (Ga and Cu isotopes). The internal fields of this contribution are assumed to be Gaussian distributed in their values, randomly oriented and static within the  $\mu\text{SR}$  time window. The parameter  $\Delta_{ns}^2/\gamma_\mu^2$  represents the second moment of this field distribution due to the nuclear spins along one Cartesian axis ( $\gamma_\mu = 2\pi \cdot 13.553\,879$  kHz/G is the gyromagnetic ratio of the muon). The second channel, described by the function  $G_{es}(t)$ , which will be discussed in detail below, represents the contribution arising from the fluctuating electronic Cu spins.

At  $T = 10$  K the muon depolarization can be satisfactorily described by assuming  $G_{es}(t) = 1$ , i.e.,  $G_{z,para}(t) = G_{KT}(t)$  with  $\Delta_{ns} = 0.16(1)$  MHz (see also Fig. 7), indicating that the fluctuations of the electronic spins are still too fast to be observed in the  $\mu\text{SR}$  time window. However, upon cooling the sample below  $T = 10$  K and down to 3.8 K, the fluctuation rate of the electronic spins decreases and the muon-spin depolarization becomes gradually dominated by the  $G_{es}(t)$  contribution. Figure 8 represents the temperature evolution of the depolarization rate  $\lambda$ . Whereas the exponent  $\beta$  remains constant in this temperature interval (i.e.,  $\beta \approx 0.78$ ), the depolarization rate exhibits a marked critical-like divergence, which must be taken as a clear evidence of the approach to a magnetic phase transition as the temperature is decreased which we associate to the occurrence of the spin-glass phase (see Figs. 1 and 6) in  $\text{CuGa}_2\text{O}_4$ .

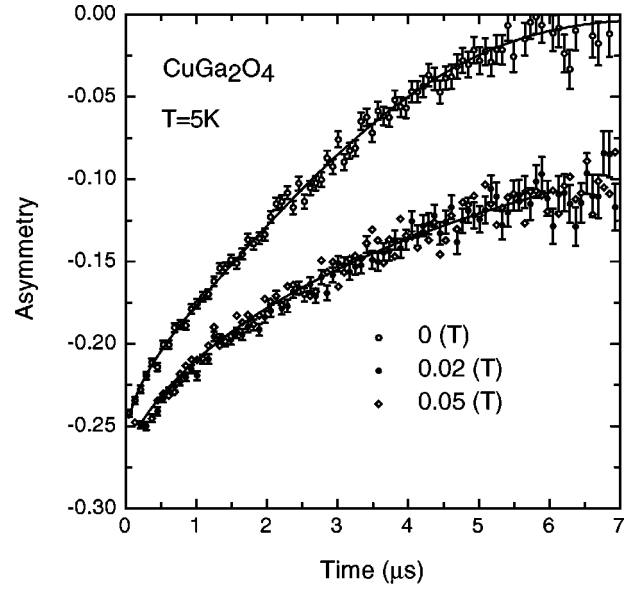


FIG. 9.  $\mu\text{SR}$  spectra measured in  $\text{CuGa}_2\text{O}_4$  at  $T = 5$  K and showing the field dependence of the asymmetry function. Whereas in zero field the depolarization function is best described according to Eq. (5), the data with applied field are only fitted by the stretched exponential term reflecting the depolarization arising from the fluctuating electronic spins (see text).

For spin-glass systems, the stretched exponential form for the electronic-spin contribution of the muon-spin depolarization function  $G_z(t)$  has been shown<sup>23</sup> to match the Kohlrausch-like stretched exponential for the local moments autocorrelation function itself, which in turn arises from a broad distribution of electronic-spin correlation times. In the particular case of moderately concentrated systems, the exponent  $\beta$  reaches the value of  $\frac{1}{3}$  at  $T_f$ . On the other hand, for conventional magnetic systems, the dynamic muon-spin depolarization function assumes an exponential form (i.e.,  $\beta = 1$ ), reflecting the unique spin-relaxation frequency of the localized moments. The situation observed here for  $\text{CuGa}_2\text{O}_4$  appears somewhat intermediate with an exponent  $\beta$  slightly, but definitively, below unity ( $\approx \frac{3}{4}$ ). This behavior is tentatively ascribed to the high concentration of local moments ( $\text{Cu}^{2+}$  ions), randomly distributed in different sublattices, for which a somewhat narrow distribution of electronic-spin correlation times could be expected.

In the temperature range between 3.8 and 10 K, the best fits with Eq. (5) provide a parameter  $\Delta_{ns}$  for the KT function (i.e., essentially the width of the internal fields arising from the nuclear moments) which is practically constant, indicating that the nuclear moments remain static at all temperatures. This is also confirmed by measurements performed in applied longitudinal fields (LF). If the nuclear moments are static within the  $\mu\text{SR}$  time window and if the applied field is sufficiently strong to quench the nuclear dipole field contribution [i.e.,  $G_{KT}(t) = 1$ ], the muon-spin depolarization should arise solely from the dynamical electronic-spin contribution and the depolarization function will assume the form  $G_z(t) = G_{es}(t)$ . This was indeed observed during LF measurements (see Fig. 9) for which a magnetic field of

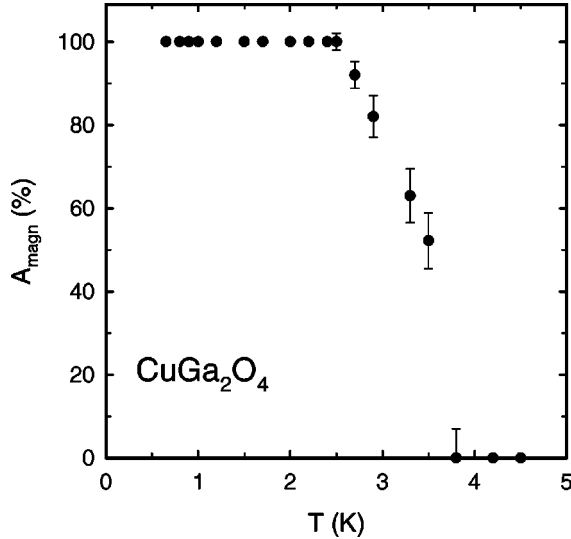


FIG. 10. Temperature dependence of the parameter  $A_{magn}$  corresponding to the magnetic volume fraction.

0.2 kOe was sufficient to quench the nuclear dipolar moments. The muon depolarization function is then well reproduced with the stretched exponential function described before, with parameters compatible with the ones extracted from the zero-field data.

For temperatures below  $T=3.8$  K, the muon depolarization increases significantly and assumes a Gaussian character at short times. For this temperature range, the best description of the data is obtained using the function

$$G_z(t) = A_{para}G_{z,para}(t) + A_{magn}G_{DKT}(t), \quad (8)$$

where  $G_{z,para}(t)$  is defined above and  $G_{DKT}(t)$  is the so-called dynamical Kubo-Toyabe (DKT) function,<sup>25</sup> which reflects that the Gaussian internal field distribution due to the occurrence of static electronic spins (second moment  $\Delta_{es}^2/\gamma_\mu^2$ ) fluctuates at the rate  $\nu$ . The first term of Eq. (8) is only present in the temperature interval between 3.8 and 2.5 K, i.e., in a region where paramagnetic domains appear to coexist with domains exhibiting static, albeit disordered, magnetic moments. Figure 10 shows the temperature evolution of the amplitude  $A_{magn}$  which mirrors the volume of the magnetic domains. Therefore it appears that in  $\text{CuGa}_2\text{O}_4$  the transition to a spin-glass state begins around  $T \approx 3.8$  K to form local clusters of frozen electronic spins which grow when the temperature is lowered and finally percolate at the same temperature where the specific anomaly is observed (i.e.,  $T \approx 2.5$  K) and which can be therefore associated to  $T_f$ .

With the exception of some limiting cases, the DKT function cannot be expressed analytically and depends directly on the parameters  $\nu$  and  $\Delta_{es}$ . Figure 11 shows the temperature dependence of the parameter  $\Delta_{es}$  which exhibits a clear increase below  $\approx 3.5$  K and can be associated to the temperature dependence of the static part of the electronic magnetic moments. The fluctuation rate  $\nu$  was found to be constant below  $T_f$  ( $\nu \approx 3.7$  MHz). It is worthwhile to note that the DKT function, which appears to describe perfectly the data for  $T \ll T_f$ , assumes a single fluctuation rate  $\nu$  for the inter-

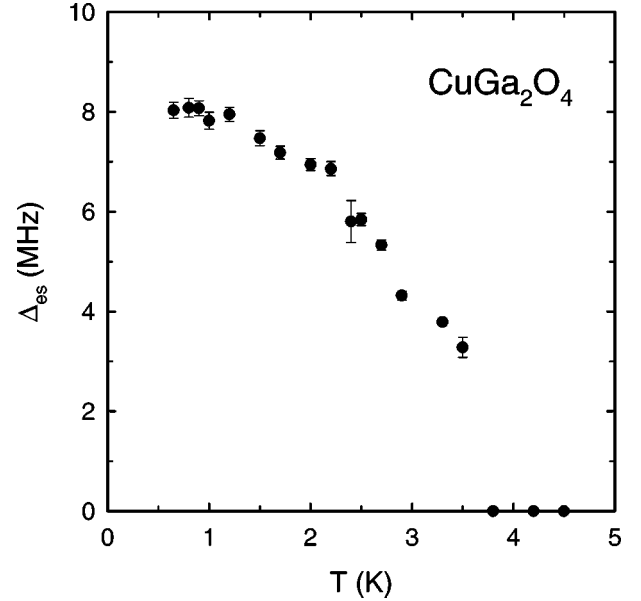


FIG. 11. Temperature dependence of the  $\Delta_{es}$  parameter of the DKT function. This parameter mirrors the width of the quasistatic field distribution below  $T_f$  and therefore the value of the quasistatic  $\text{Cu}^{2+}$  moment.

nal fields sensed by the muon spin. This has to be connected to our simple picture that the slightly reduced value in the paramagnetic phase of the exponent  $\beta$  compared to unity must be related to a rather narrow distribution of electronic-spin correlation times.

## VI. MONTE CARLO SIMULATIONS

The experimental observations presented in the preceding sections all indicate that the  $\text{Cu}^{2+}$  magnetic moments in  $\text{CuGa}_2\text{O}_4$  undergo a phase transition to a spin-glass state at  $T_f=2.5$  K. To understand the nature of this magnetic state, Monte Carlo simulations were performed using a model of Heisenberg spins with competing exchange interactions including random anisotropies. These arise as the result of Jahn-Teller distortions of the octahedrons and tetrahedrons surrounding the  $\text{Cu}^{2+}$  positions.<sup>17</sup> The local distortions occur randomly along one of the three equivalent  $C_4$  cubic axes. Consequently, the exchange interactions between nearest-neighbors spins located on tetrahedral ( $A$  sites) and octahedral ( $B$  sites) positions have tetragonal anisotropy. However, the direction of the tetragonal axis is random in a crystal with cubic symmetry. For the model calculations, we considered exchange interactions between nearest neighbors  $\text{Cu}^{2+}(A) - \text{Cu}^{2+}(B)$  and second-nearest-neighbors  $\text{Cu}^{2+}(B) - \text{Cu}^{2+}(B)$  magnetic ions. We took into account the fact that in the spinel lattice the  $\text{Cu}^{2+}$  ions are randomly distributed between the  $A$  and  $B$  sites with occupation probabilities of 25 and 75%, respectively. Consequently, the model Hamiltonian for this spin system is given by

$$\mathbf{H} = - \sum_{\alpha=x,y,z} \sum_{i,j} J_{ij}^{\alpha\alpha} S_i^\alpha S_j^\alpha P_i^0 P_j^0 - \sum_{i,j} K_{ij} S_i S_j P_i^0 P_j^0 - \sum_i H S_i^z P_i^0, \quad (9)$$

where the  $J_{ij}^{\alpha\alpha}$ 's represent the exchange integrals between the nearest-neighbors  $\text{Cu}^{2+}$  ions located in the  $A$  and  $B$  sites;  $K_{ij}$  is the exchange parameter between nearest-neighbors  $\text{Cu}^{2+}$  ions on the octahedral sublattice and  $H$  the external magnetic field. The components of the exchange interactions  $J_{ij}^{\alpha\alpha}$  are distributed randomly with the same probability, namely

$$\begin{aligned} P(J_{ij}^{xx}, J_{ij}^{yy}, J_{ij}^{zz}) = & 1/3 \delta(J_{ij}^{xx} - J_0 - \Delta J) \delta(J_{ij}^{yy} - J_0) \delta(J_{ij}^{zz} - J_0) \\ & + 1/3 \delta(J_{ij}^{xx} - J_0) \delta(J_{ij}^{yy} - J_0 - \Delta J) \\ & \times \delta(J_{ij}^{zz} - J_0) + 1/3 \delta(J_{ij}^{xx} - J_0) \delta(J_{ij}^{yy} - J_0) \\ & \times \delta(J_{ij}^{zz} - J_0 - \Delta J), \end{aligned} \quad (10)$$

where  $\delta(x)$  is the  $\delta$  function. The random numbers  $P_i^t$  and  $P_j^0$  determine the distribution  $\mathbf{P}$  of the  $\text{Cu}^{2+}$  ions among the tetrahedral and octahedral sites in the spinel lattice, respectively, so that

$$\mathbf{P}(P_i^{t,0}) = \nu^{t,0} \delta(P_i^{t,0} - 1) + (1 - \nu^{t,0}) \delta(P_i^{t,0}) \quad (11)$$

with  $\nu^t = 0.25$  and  $\nu^0 = 0.75$ . The Monte Carlo simulations were carried out using periodic boundary conditions for a lattice consisting of  $24 \times 24 \times 24$  sites and over 30 000–60 000 MK steps per spins. We calculated the magnetization of the spin lattice, the magnetic susceptibility, and the spin-spin correlation function  $\langle S(0)S(R) \rangle$ . We simulated the temperature dependence of the EA-order parameter  $q(T)$  for the  $A$  and  $B$  spins, respectively, defined as

$$q^{\alpha\beta} = (1/N_\beta) \sum_{i=1}^{N_\beta} \langle S_i^\alpha \rangle^2, \quad \alpha = x, y, z, \quad \beta = t, 0. \quad (12)$$

Here  $N_\beta$  is the number of spins in the  $A$  and  $B$  sites. The susceptibility  $\chi$  is defined in zero external field as follows:

$$\begin{aligned} \chi J_0 = & \left[ \left\langle \left( (1/N_A) \sum_{i \in A} S_i^A - (1/N_B) \sum_{i \in B} S_i^B \right)^2 \right\rangle \right. \\ & \left. - \left\langle (1/N_A) \sum_{i \in A} S_i^A - (1/N_B) \sum_{i \in B} S_i^B \right\rangle^2 \right] / (T/J_0), \end{aligned} \quad (13)$$

where  $i$  is summed over octahedral ( $B$ ) and tetrahedral ( $A$ ) sites consisting of  $N_A$  and  $N_B$  spins. The susceptibility in nonzero field is

$$\chi J_0 = \left[ \left\langle (1/N_A) \sum_{i \in A} S_i^A - (1/N_B) \sum_{i \in B} S_i^B \right\rangle \right] / (H/J_0). \quad (14)$$

The exchange parameters  $\Delta J$ ,  $K$ , and  $J_0$  were obtained by fitting the Monte Carlo results to the experimental freezing temperature  $T_f$ , the paramagnetic Néel temperature  $\Theta$  (K) and the magnetic field dependence of the magnetization  $M(H)$ . Figure 12 shows the temperature dependence of the magnetic susceptibility calculated by the Monte Carlo method for two values of magnetic fields,  $H=0$  Oe and  $H=10^4$  Oe, respectively. In agreement with the experimental results, the calculated magnetic susceptibility exhibits a

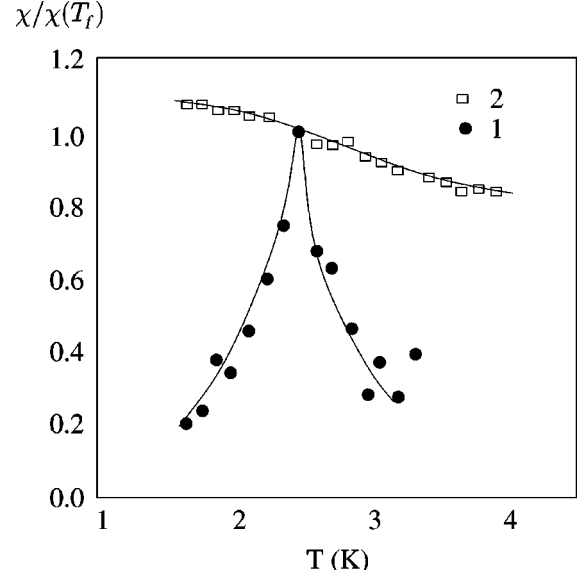


FIG. 12. Temperature dependence of the normalized magnetic susceptibility for values of magnetic fields  $H=0$  Oe and  $H=10^4$  Oe (curves 1 and 2, respectively) with exchange constants  $J = -12$  K,  $K = -6$  K, and  $\Delta J = -1.2$  K.

sharp cusp at  $T_f \approx 2.5$  K which is suppressed when a magnetic field is applied. The value of the cusp is attributed to long-wavelength spin correlations. According to the Monte Carlo results the expanded short-range order exists at a distance of four lattice constants where the spin-spin correlation function has decreased three times. It differs from the usual spin glass.

As shown in Fig. 13 the EA-order parameters for both the  $A$  and  $B$  sublattice sharply increase below  $T = T_f$ . Moreover, the spin-spin correlation function  $\langle S(0)S(L/2) \rangle$  ( $L = \text{Monte Carlo sample size}$ ) reveals the absence of any long-range magnetic ordering in the spin system. The Monte Carlo re-

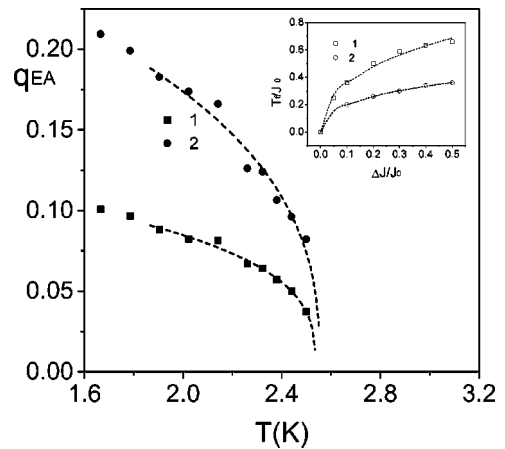


FIG. 13. (a) Temperature dependence of the Edwards-Anderson parameter  $q(T)$  for the  $A$  (curve 1) and  $B$  (curve 2) sublattices, respectively, as simulated with Monte Carlo. Inset: Dependence of the freezing temperature  $T_f$  on exchange anisotropy  $\Delta J/J_0$  for  $K/J_0 = 0.5$  (curve 1) and  $K/J_0 = 0.5$  (curve 2) obtained from Monte Carlo simulation.

sults show that for the concentrations of  $\text{Cu}^{2+}$  spins of relevance for  $\text{CuGa}_2\text{O}_4$ , the crystal is in a superparamagnetic state when  $\Delta J=0$ . Introducing random anisotropy for the exchange interaction  $J$  results in a spin cluster blocking at the freezing temperature  $T_f$ . In that respect, we note that the exchange anisotropy leads to increasing the freezing temperature as shown in inset of Fig. 13. To reproduce the magnetization data in a satisfactory way, we found it necessary to give a nonzero value to the antiferromagnetic exchange interaction  $K$  which decreases the  $T_f$  as result of competing of the interactions  $K$  and  $J$ . The field dependence of the magnetization exhibits a non-linear dependence against the magnetic field. The increase of the exchange parameter  $K$  leads to a decrease of the nonlinearity of  $M(H)$ . From a least-square refinement of the field dependence of the magnetization at  $T=1.8$  K we obtained the parameter values  $\Delta J/J_0=0.1$ ,  $K/J_0=0.5$  (see Fig. 4). The exchange parameter  $J_0$ , as determined from the freezing temperature  $T_f$ , from the paramagnetic susceptibility in the temperature range  $90 \leq T \leq 160$  K and from the magnetization curve, amounts to  $-12$ ,  $-12.5$ , and  $-13$  K, respectively. Therefore the mean values of the model parameters are  $J=-12.5$  K,  $\Delta J=-1.3$  K, and  $K=-6.2$  K.

## VII. CONCLUSION

We have presented magnetization, magnetic susceptibility, specific-heat, and  $\mu\text{SR}$  measurements in  $\text{CuGa}_2\text{O}_4$ . The data are consistent with a spin-glass transition of the copper sublattice below  $T_f$  in this material. In particular, we observe a cusp in the temperature dependence of the magnetic sus-

ceptibility at  $T_f \approx 2.5$  K which is suppressed when a magnetic field is applied. A pronounced hysteresis is observed in the temperature dependence of the magnetic susceptibility for zero-field-cooled and field-cooled samples. The muon-spin relaxation measurements have shown that above the freezing temperature, the asymmetry function is described by the stretched exponential typical of disordered systems. However, the value of the exponent  $\beta$  points to a narrow distribution of correlation times of the local moments. The temperature dependence of the magnetic volume fraction indicates that in  $\text{CuGa}_2\text{O}_4$  the transition to a spin-glass state begins around  $T \approx 3.8$  K to form locally clusters of frozen spins which grow when the temperature is lowered and finally percolate around  $T_f \approx 2.5$  K. By means of Monte Carlo simulations we were able to reproduce the main features of the magnetic susceptibility and of the magnetization curve measured in  $\text{CuGa}_2\text{O}_4$ . The results of Monte Carlo simulations show that the Jahn-Teller effect plays an essential role in forming the magnetic ground state as it introduces random anisotropy in the exchange interactions between the copper ions. With the added effect of random distribution of cations in the spinel structure this leads to the formation of a spin-glass state in  $\text{CuGa}_2\text{O}_4$ . Using a realistic spin model which takes into account the effective distribution of the  $\text{Cu}^{2+}$  ions in the spinel structure, reliable exchange parameters could be obtained for  $\text{CuGa}_2\text{O}_4$ .

## ACKNOWLEDGMENTS

This work was partially supported by an INTAS-97-0177 grant and by the MAT99/1142 project.

\*On leave of absence in the Kamerlingh Onnes Laboratorium, Leiden University, The Netherlands.

<sup>1</sup> K.H. Fisher and J.A. Hertz, *Spin Glasses*, Cambridge Studies in Magnetism (Cambridge University Press, Cambridge, England, 1991).

<sup>2</sup> K.H. Fisher, *Phys. Status Solidi A* **16**, 357 (1983).

<sup>3</sup> J. Souletie, *J. Phys. (France)* **39**, C2-3 (1978).

<sup>4</sup> M.A. Ruderman and C. Kittel, *Phys. Rev.* **96**, 99 (1954); T. Kasuya, *Prog. Theor. Phys.* **16**, 45 (1956); K. Yosida, *Phys. Rev.* **106**, 893 (1957).

<sup>5</sup> H.G. Bohn, W. Zinn, B. Dorner, and A. Kollmar, *Phys. Rev. B* **22**, 5447 (1980).

<sup>6</sup> H. Maletta and P. Convert, *Phys. Rev. Lett.* **42**, 108 (1979).

<sup>7</sup> S.F. Edwards and P.W. Anderson, *J. Phys. F: Met. Phys.* **5**, 965 (1975).

<sup>8</sup> L. de Seze, *J. Phys. C* **10**, L353 (1977).

<sup>9</sup> J. Villain, *Z. Phys. B* **33**, 31 (1979).

<sup>10</sup> M. Sparks, in *Ferromagnetic Relaxation Theory* (McGraw-Hill, New York, 1964).

<sup>11</sup> P.W. Anderson, *Phys. Rev.* **102**, 1008 (1956).

<sup>12</sup> C.P. Pool, Jr. and H.A. Farach, *Z. Phys. B: Condens. Matter* **47**, 55 (1982).

<sup>13</sup> D. Fiorani, S. Viticoli, J.L. Dormann, J.L. Tholence, and A.P. Murani, *Phys. Rev. B* **30**, 2776 (1984).

<sup>14</sup> Z. Popovic and S. Satpathy, *Phys. Rev. Lett.* **84**, 1603 (2000).

<sup>15</sup> Guo-meng Zhao, K. Conder, H. Keller, and K.A. Müller, *Nature (London)* **381**, 676 (1996).

<sup>16</sup> A. Shengelaya, Guo-meng Zhao, C.M. Aegerter, K. Conder, I.M. Savić, and H. Keller, *Phys. Rev. Lett.* **24**, 5142 (1999).

<sup>17</sup> K. Kugel and D. Khomsky, *Usp. Fiz. Nauk* **136**, 621 (1982) [*Sov. Phys. Usp.* **25**, 231 (1982)].

<sup>18</sup> J.M.R. Gonzales and C.O. Arena, *J. Chem. Soc. Dalton Trans.* **1985**, 2155 (1985).

<sup>19</sup> W.E. Fogle, J.D. Boyer, R.A. Fisher, and N.E. Phillips, *Phys. Rev. Lett.* **50**, 1815 (1983).

<sup>20</sup> S. Kirkpatrick, *Phys. Rev. Lett.* **36**, 69 (1976).

<sup>21</sup> J.A. Mydosh, *Spin Glasses: An Experimental Introduction* (Taylor and Francis, London, 1993).

<sup>22</sup> K. Emmerich, E. Lippelt, R. Neuhaus, H. Pinkvos, Ch. Schwink, F.N. Gygax, A. Hintermann, A. Schenck, W. Studer, and A.J. van der Wal, *Phys. Rev. B* **31**, 7226 (1985).

<sup>23</sup> I.A. Campbell, A. Amato, F.N. Gygax, D. Herlach, A. Schenck, R. Cywinski, and S.H. Kylcoyne, *Phys. Rev. Lett.* **72**, 1291 (1994); A. Kerren, P. Mendels, I.A. Campbell, and J. Lord, *ibid.* **77**, 1386 (1996).

<sup>24</sup> J.R. Stewart and R. Cywinski, *Phys. Rev. B* **59**, 4305 (1999), and references therein.

<sup>25</sup> R. Kubo, *Hyperfine Interact.* **8**, 731 (1981).